JOURNAL OF PROPULSION AND POWER
Vol. 26, No. 5, September–October 2010

Separating Direct and Indirect Turbofan Engine Combustion Noise Using the Correlation Function

Jeffrey Hilton Miles*
NASA John H. Glenn Research Center at Lewis Field, Cleveland, Ohio 44135

DOI: 10.2514/1.48908

A previous investigation on the presence of direct and indirect combustion noise for a full-scale turbofan engine using a far-field microphone at 130° is extended by also examining signals obtained at two additional downstream directions using far-field microphones at 110 and 160°. A generalized cross-correlation function technique is used to study the change in propagation time to the far field of the combined direct and indirect combustion noise signal as a sequence of low-pass filters is applied. The filtering procedure used produces no phase distortion. As the low-pass-filter frequency is decreased the travel time increases because the relative amount of direct combustion noise is reduced. The indirect combustion noise signal travels more slowly because in the combustor entropy fluctuations move with the flow velocity, which is slow compared to the local speed of sound. The indirect combustion noise signal travels at acoustic velocities after reaching the turbine and being converted into an acoustic signal. The direct combustion noise is always propagating at acoustic velocities. The results show that time delays measured at each angle are fairly consistent with one another for a relevant range of operating conditions and demonstrate source separation of a mixture of direct and indirect combustion noise. The results may lead to a better idea about the acoustics in the combustor and may help develop and validate improved reduced-order physics-based methods for predicting turbofan engine core noise.

Nomenclature

B_e	=	resolution bandwidth, Hz, $1/T_d = r_s/N = 2$ Hz
c_c	=	speed of sound in combustor, m/s
c_o	=	ambient speed of sound, m/s
D	=	propagation-time delay or lag, s
f_c	=	upper frequency limit, $1/2\Delta t = r_s/2$, Hz (32,768 Hz)
f_L	=	cutoff frequency of low-pass filter
L_c	=	cooled length in combustor, 0.095 m
L_y	=	number of frequencies, $f_c/\Delta f = N/2$ (16,384)
N	=	segment length, number of data points per segment (32,768)
$\Re$	=	molar gas constant, 8.3145 J/mole°K
R_x	=	autocorrelation function
R_{xy}	=	cross-correlation function
r	=	microphone radial location, m (30.48 m)
r_s	=	sample rate, samples/s (65,536)
T_c	=	turbine inlet temperature, K
$T_d(i)$	=	record length of segment i, N/r_s, 0.5 s
T_{total}	=	total record length, s (≈70 s)
t	=	time, s
v_s	=	typical flow speed in combustor, 30 m/s
W	=	molar mass of air, 0.029 kg/mol
x	=	time-dependent signal
y	=	time-dependent signal
γ	=	specific heat ratio or adiabatic index, 1.4
γ^2_{nn}	=	magnitude-squared coherence function of noise
γ^2_{xy}	=	magnitude-squared coherence function of signals x and y
Δf	=	frequency step, $1/T_d = r_s/N$, Hz (2 Hz)
Δt	=	sampling interval, $1/r_s$ (1/65,536), s
$\Delta\tau(f_L)\|_{\text{peak}}$	=	time-delay peak using low-pass filter f_L relative to peak using no filter, s
ρ_{xy}	=	cross-correlation coefficient
τ	=	time, s
τ_d	=	direct combustion noise signal travel time, s
τ_{duct}	=	noise signal travel time in the duct, s
τ_i	=	indirect combustion noise signal travel time, s

Subscript

i	=	running segment index

I. Introduction

COMBUSTION noise can make a significant contribution to overall turbofan engine noise at low-power settings, which are typical of approach flight. In addition, technological advancement in aircraft engine-cycle design and noise-reduction methods may reduce jet and fan noise even at higher engine power points, where they currently are of more importance than combustion noise. With the pending development of reduced-gaseous-emission aircraft engine combustors, the gaps in combustor source knowledge have increased in importance. Consequently, the prediction and measurement of combustion noise is an area of increased interest.

The low-frequency contribution of combustion noise, both direct and indirect, is a unique characteristic feature of combustion noise and differentiates it from fan and jet noise. Combustion noise is difficult to study because hydrodynamic and acoustic pressure fluctuations are intermixed at the source location. Taking measurements at the source location is also challenging due to the combustor environment. In addition, much of the far-field noise is not correlated with the combustor and/or turbine internal noise. However, the part that is correlated can be studied using signal cross-correlation functions and coherence functions. Studying this part can improve our understanding of the acoustics in combustors and may ultimately enable development of improved reduced-order physics-based methods for predicting direct and indirect combustor noise.

Cross-correlation functions were used by Miles [1] with low-pass filters to investigate direct and indirect combustion noise source separation based on signal propagation-time delays. Using the cross-correlation function, time delays were identified in all cases, clearly indicating that the combustor is the source of the noise. The

Presented as Paper 2010-19 at the 48th AIAA Aerospace Sciences Meeting, Orlando, FL, 4–7 January 2010; received 13 January 2010; revision received 10 May 2010; accepted for publication 23 May 2010.

*Aerospace Engineer, Acoustics Branch, 21000 Brookpark Road; Associate Fellow AIAA.

low-frequency noise is a blend of indirect combustion noise (which is loudest in the 0–200 Hz frequency range) and direct combustion noise (which is loudest in the 200–400 Hz frequency range) for this engine. Consequently, far-field microphone signals at 130° that are unfiltered or low-pass-filtered at a frequency of 400 Hz so that the edge frequency of the passband is 400 Hz had a cross-correlation time delay near 90 ms, while the same signals are low-pass-filtered at frequencies less than 400 Hz so that the edge frequency of the passband is less than 400 Hz had a cross-correlation time delay longer than 90 ms. Low-pass filtering at frequencies less than 400 Hz partially removes mainly the direct combustion noise signals. The remainder includes the indirect combustion noise signal, which travels more slowly because of the dependence on the entropy convection velocity in the combustor. Source separation of direct and indirect combustion noise was demonstrated by proper use of low-pass filters with the cross-correlation function for the same range of operating conditions used herein: namely, 48, 54, 60, and 71% of maximum power. The previous investigation used a combustor pressure sensor and a far-field microphone at 130° to study the change in delay time with the low-pass-filter frequency and operating condition. In this report, the study is extended by using far-field microphones at 110 and 160°.

This cross-correlation function procedure is applied to data from a dual-spool TECH977 turbofan engine. Acoustic data from the same TECH977 engine test program are discussed by Miles [2,3], Mendoza et al. [4], Weir and Mendoza [5], Schuster [6], Royalty and Schuster [7], Dougherty and Mendoza [8], Weir [9], and Hultgren and Miles [10].

The research discussed herein is an extension of the study of the combustion noise of the TECH977 engine conducted by Miles [2,3], using a cross-spectrum phase-angle procedure and the cross-correlation function procedure used by Miles [1]. These reports indicate that for this particular engine combustion noise occurs primarily in the 0–400 Hz frequency range. Miles [1] also discusses previous relevant work in detail.

The fundamental premise of this report and Miles [1] is that filtering to remove frequencies above 400 Hz leaves the combined direct and indirect combustion noise unchanged in the signal. Filtering to remove frequencies above 200 Hz leaves the indirect combustion noise mostly unchanged. In addition, the low-pass filters are designed to eliminate phase-angle modifications and to leave the signal delay time identified as the location of peak of the correlation function of random noise at the proper time value. Results are presented for an unfiltered condition and after low-pass filtering to remove frequencies above 400, 300, 200, 150, and 100 Hz using a filtering procedure having no phase distortion. The idea of prefiltering the signals before doing a cross-correlation is discussed by Carter [11] and Scarbrough et al. [12], and the resulting function is identified as a generalized cross-correlation (GCC) function. However, any phase distortion produced by the filters used by Carter [11] and Scarbrough et al. [12] to create the GCC function they use does not appear to be a problem, since it is not discussed in these papers. A special procedure is used herein to ensure that no phase distortion is introduced.

II. Engine Noise Data and Analysis

A. Engine Test Data

The static engine test was conducted at Honeywell's San Tan outdoor acoustic test facility. A polar array of 32 ground-plane microphones was used. Each B&K 4134 microphone in an inverted stand with a 7 mm ground spacing was placed on a 100 ft radius. The microphones were positioned from 5 to 160° (relative to the inlet) in 5° increments. The microphone array is shown in [2,4,5,9].

The dual-spool turbofan engine has a direct-drive wide-chord fan connected by a long shaft to the low-pressure turbine spool and a high-pressure compressor connected by a concentric short shaft to the turbine high-pressure spool. The fan diameter is 34.2 in. The combustor design is a straight-through-flow annular geometry with 16 fuel nozzles and two igniters. One of the igniters is replaced by a pressure transducer, which is identified herein as CIP1. The dependent source-separation technique used to identify direct and indirect combustion noise uses data from the CIP1 transducer and far-field microphones at 110 and 160°. Engine diagrams are shown in [2,4,5,7–9].

The data acquisition system had a sampling rate of 65,536 Hz and a sampling duration of roughly 70 s. This permitted data reduction using 254 overlapped ensemble averages at a bandwidth resolution of 2 Hz. Further signal estimation parameters are shown in Table 1. Autospectra, coherent output power, aligned and unaligned coherence, aligned cross-spectra, and aligned and unaligned spectra are shown in [2].

B. Correlation Functions

The autocorrelation function describes the general dependence of the values of data at one time on the value at another time. The autocorrelation function is

$$R_{xx}(\tau) = \lim_{T\to\infty} \frac{1}{T} \int_0^T x(t)x(t+\tau)\,\mathrm{d}t \tag{1}$$

The cross-correlation function describes the general dependence of the values of one set of data at one time on the value of another set of data at another time. The cross-correlation function is

$$R_{xy}(\tau) = R_{yx}(-\tau) = \lim_{T\to\infty} \frac{1}{T} \int_0^T x(t)y(t+\tau)\,\mathrm{d}t \tag{2}$$

Note that the cross-correlation function is not symmetric in time about zero.

The normalized cross-correlation function known as the cross-correlation function coefficient (normalized cross-covariance function) used herein to plot the cross-correlation functions is defined as

$$\rho_{xy}(\tau) = \rho_{yx}(-\tau) = \frac{R_{xy}(\tau)}{\sqrt{R_{xx}(0)R_{yy}(0)}} \tag{3}$$

by Bendat and Piersol [13,14]. While the total cross-correlation functions are calculated, only the positive time delay is shown.

C. Filtering

The 100, 200, 300, and 400 Hz low-pass filters used are three-section Butterworth filters. The filters will be identified herein by the low-pass-filter cutoff frequency f_L. Filter design was done using bilinear transformation following a method described by Stearns and David [15]. These filter parameters are given in Tables 2, 4, 5, and 6 of the report by Miles [1] on applying the procedure discussed herein to signals from the 130° far-field microphone.

To see if the results depended on the filter design approach, a non-Butterworth filter was used as a 150 Hz low-pass filter with coefficients shown in Table 3 of the report by Miles [1]. For the first section, this filter uses the second-section filter values of the 300 Hz low-pass filter shown in Table 5 of the report by Miles [1]. For the second and third sections, this filter uses the third-section filter values

Table 1 Spectral estimate parameters

Parameter	Value
Segment length (data points per segment) N	32768
Sample rate r_s, samples/s	65,536
Segment length $T_d = N/r_s$, s	0.500
Sampling interval $\Delta t = 1/r_s$, s	1/65,536
Bandwidth resolution $B_e = \Delta f = 1/T_d = r_s/N$, Hz	2.0
Upper frequency limit $f_c = 1/2\Delta t = r_s/2$, Hz	32,768
Number of frequencies $Ly = f_c/\Delta f = N/2$	16384
Propagation-time delay/lag ($T = 9°$C, $r = 30.48$ m) $D = 5927/65,536$, s	0.09044
Number of independent samples n_s	128
Overlap	0.50
Sample length T_{total}, s	≈70

of the 300 Hz filter shown in Table 5 of the report by Miles [1]. The 150 Hz filter has a larger transition band than a properly designed Butterworth filter.

To make certain that the filters introduce no phase-angle modification, the filter for each segment is applied to the forward time series and then again with the time reversed. The time-series reversal is then removed before processing the next segment or quitting. This procedure is discussed by Kormylo and Jain [16] and by Hamming [17]. Note the effective filter function is the square of the absolute value of the designed filter function.

To demonstrate the filtering process a study was conducted using white noise generated by use of a Mersenne Twister random number generator [18]. Figure 1 of the paper by Miles [1] presenting results obtained using the 130° far-field microphone also shows the effect of each filter on the signal amplitude.

III. Results

The sequence of low-pass filters, discussed in the previous section, is applied to the combustor pressure transducer signal and far-field microphone signal. The signal resulting from using the 400 Hz low-pass filter contains both indirect and direct combustion noise. By applying further low-pass filters in the sequence, i.e., 300, 200, 150, and 100 Hz, the resulting signal will have a decreasing amount of direct combustion noise. The signal resulting from using the 100 Hz low-pass filter contains mainly indirect combustion noise.

The cross-correlation functions between the microphone at 110° and the combustor pressure sensor are presented in Figs. 1–4, and the cross-correlation functions between the microphone at 160° and the combustor pressure sensor are presented in Figs. 5–8. The figures show the cross-correlation functions in the time region, which contain the peak value. The left side of the peak is determined by the direct combustion noise, which moves at acoustic speeds along its full path. The right side of the peak in the region is controlled by the indirect combustion noise, which initially propagates with the mean flow velocity. The combustion noise spectrum has a limited frequency range. For this particular engine, this limit is about 400 Hz.

The cross-correlation of band-limited signals is smeared in the time domain. An example is shown in Fig. 2 of the report by Miles [1], in which various low-pass filters are used with white noise. Consequently, all the cross-correlation function show smeared peaks.

Figures 1–8 show that as the low-pass-filter cutoff frequency f_L is decreased, more direct combustion noise (which controls the left side of the peak) is removed, the temporal smearing is increased, and the peak occurs at a longer time delay.

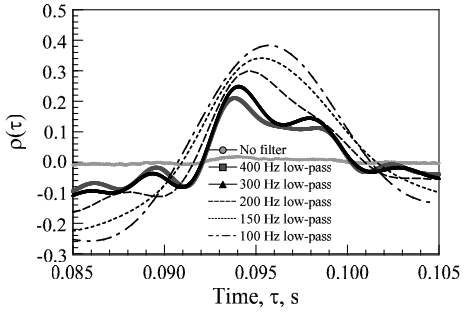

a) 100-400 Hz low-pass filters

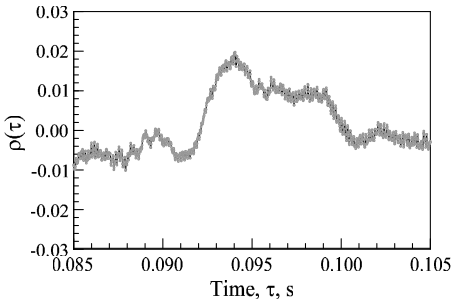

b) No filter

Fig. 1 Normalized cross-correlation using internal combustor pressure sensor and 110° far-field microphone calculated using no filter and various low-pass filters at setting of 48% of maximum power in region of peak values.

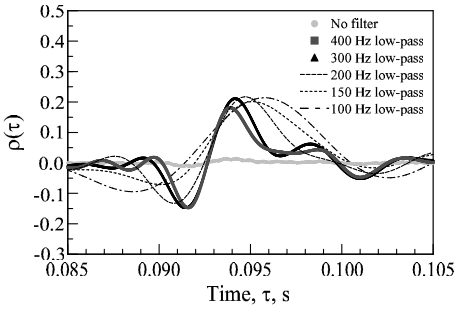

a) 100-400 Hz low-pass filters

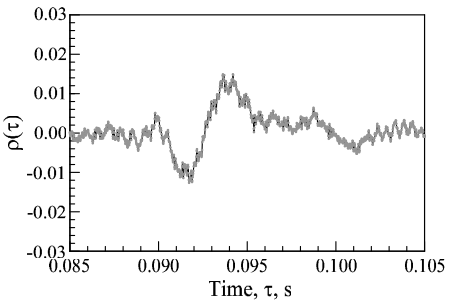

b) No filter

Fig. 2 Normalized cross-correlation using internal combustor pressure sensor and 110° far-field microphone calculated using no filter and various low-pass filters at setting of 54% of maximum power in region of peak values.

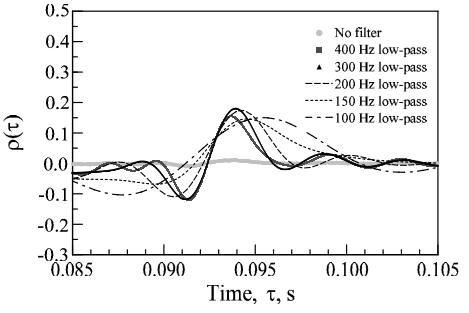

a) 100-400 Hz low-pass filters

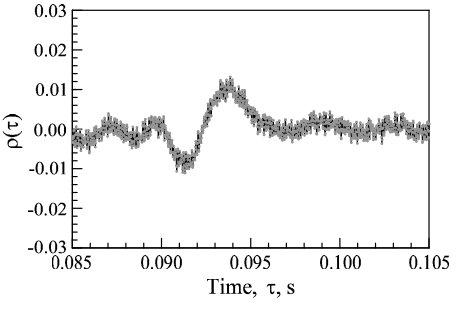

b) No filter

Fig. 3 Normalized cross-correlation using internal combustor pressure sensor and 110° far-field microphone calculated using no filter and various low-pass filters at setting of 60% of maximum power in region of peak values.

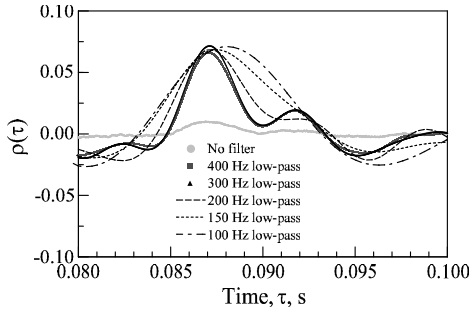

a) 100-400 Hz low-pass filters

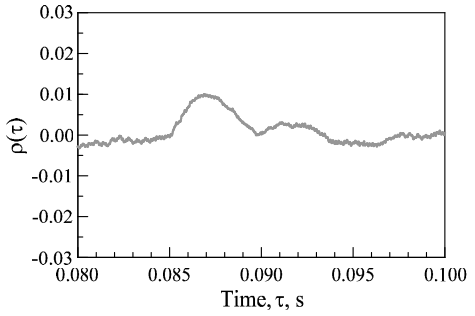

b) No filter

Fig. 4 Normalized cross-correlation using internal combustor pressure sensor and 110° far-field microphone calculated using no filter and various low-pass filters at setting of 71% of maximum power in region of peak values.

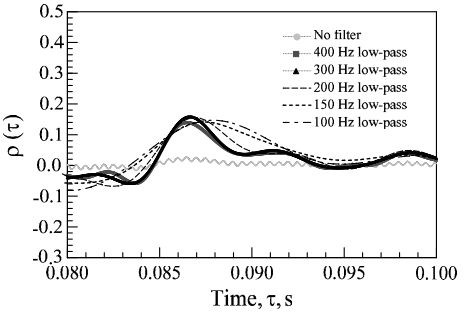

a) 100-400 Hz low-pass filters

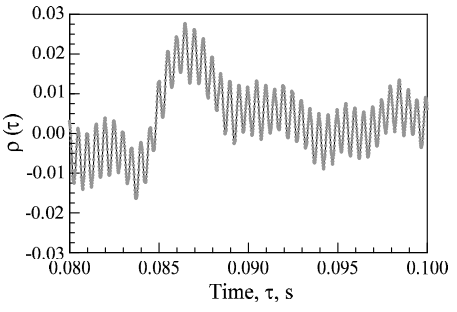

b) No filter

Fig. 6 Normalized cross-correlation using internal combustor pressure sensor and 160° far-field microphone calculated using no filter and various low-pass filters at setting of 54% of maximum power in region of peak values.

Unfiltered and low-pass-filtered cross-correlation functions between a combustor pressure sensor and a far-field microphone at 110 and 160° at the 54, 60, and 71% of maximum-power settings showed a single time-delay peak. However, at the 48% of maximum-power setting a single or double peak was observed, depending on the low-pass-filter cutoff frequency. The 48% operating condition cross-correlation functions showed a double peak when using unfiltered and filtered signals with cutoff frequencies of 300 and 400 Hz.

For the unfiltered cross-correlation and the cross-correlation filtered using a 400 Hz cutoff frequency at each power setting, the largest peak is at an acoustic time delay near 94 ms for the 110° far-field microphone case, near 90 ms for the 130° far-field microphone case (see Miles [1]), and near 86.5 ms for the 160° far-field

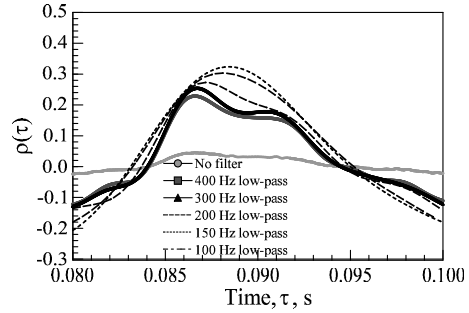

a) 100-400 Hz low-pass filters

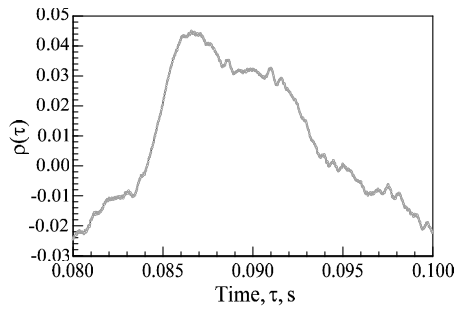

b) No filter

Fig. 5 Normalized cross-correlation using internal combustor pressure sensor and 160° far-field microphone calculated using no filter and various low-pass filters at setting of 48% of maximum power in region of peak values.

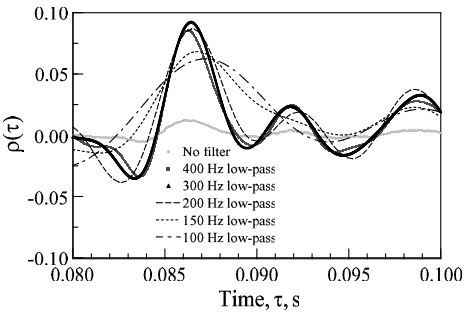

a) 100-400 Hz low-pass filters

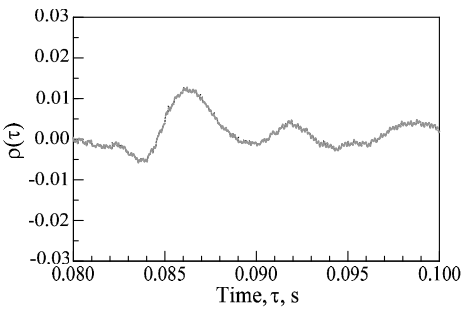

b) No filter

Fig. 7 Normalized cross-correlation using internal combustor pressure sensor and 160° far-field microphone calculated using no filter and various low-pass filters at setting of 60% of maximum power in region of peak values.

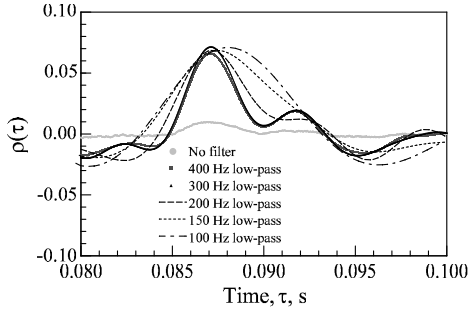

a) 100-400 Hz low-pass filters

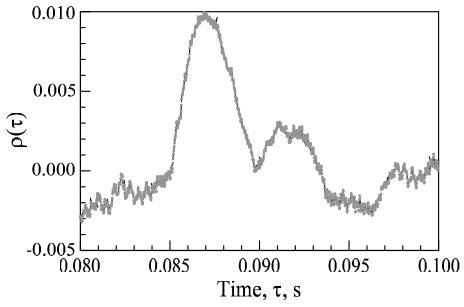

b) No filter

Fig. 8 Normalized cross-correlation using internal combustor pressure sensor and 160° far-field microphone calculated using no filter and various low-pass filters at setting of 71% of maximum power in region of peak values.

microphone case. For the double-peak case at the 48% operating condition, the second peak is near 98 ms for the 110° far-field microphone case, near 95 ms for the 130° far-field microphone case (see Miles [1]), and near 91 ms for the 160° far-field microphone case. Consequently, the time delay using this process is 4 ms for the case using the 110° far-field microphone, 5 ms for the case using the 130° far-field microphone, and 4.5 ms for the case using the 160° far-field microphone.

A double peak is shown in Figs. 1 and 5 for the 48% of maximum-power case. The highest peak in the cross-correlation of the unfiltered signals is due to the acoustic propagation time. The second peak may be due to the acoustic propagation time of the indirect combustion noise or it may be due to some engine-related interference factor. To avoid subjective observations, this study is based on using the filtering of the signals to change the ratio of acoustic signals due to direct combustion noise and acoustic signals due to indirect combustion noise. This is nonsubjective and facility-independent. Filtering without introducing any phase shift does not change the propagation physics of the acoustic signals or entropy signals. The presence of the two peaks for the 48% of maximum-power case cannot be avoided. However, they are not a feature present at all power settings. The filtering procedure can be applied at all power settings. Regardless, the location of the double-peak or single-peak maximum value shifts to larger time delays as the low-pass-filter cutoff frequency is decreased, and this fact is an observable phenomenon.

At the three higher operating conditions, the two-peak phenomenon is not observed in cross-correlations made using the combustor pressure sensor with the 110 and 160° far-field microphones. Only a single-peak cross-correlation is observed. The reason that only a single peak is detected is not clear, but it is possible that the relative amount of indirect combustion noise in the signal is decreased, thus making its detection as a discrete peak more difficult at these three higher power settings. Another possibility is that the ripple that is observed at the 48% operating condition is due to a convective entropy feedback mechanism, which acts to enhance the indirect combustion noise signal for this case. However, in all cases the single peak or the left peak where a double peak occurs shifts to the right as the low-pass-filter cutoff frequency is decreased.

The resulting delay time values of the peaks and the peak values of the normalized cross-correlation function for the 110° far-field microphone case are shown in Tables 2 and 3. The resulting delay time values of the peaks and the peak values of the normalized cross-correlation function for the 160° far-field microphone case are shown in Tables 4 and 5.

IV. Discussion

A. Dependent Source Separation

An interpretation of the time delay for the peaks of the cross-correlation function shown in Tables 2 and 4 for the 110 and 160° far-field microphones and in Table 7 of [1] for the 130° far-field microphone can be made by plotting the relative time-delay peaks of the cross-correlation functions, $\Delta\tau_{f_L}|_{\text{peak}}$. Two procedures are used herein to obtain a reference time delay. One procedure uses the time-delay peak when the signals are analyzed with no filter. The second procedure uses the time-delay peak when the signals are analyzed with the 400 Hz low-pass filter:

$$\Delta\tau(f_L)|_{\text{peak}} = \tau(f_L)|_{\text{peak}} - \tau(\text{reference})|_{\text{peak}}, \text{ms} \tag{4}$$

These plots are shown two ways. In Fig. 9 for each angle the variation of $\Delta\tau(f_L)|_{\text{peak}}$ as a function of f_L for each power setting is shown using the no-filter value as the reference. This produces

Table 2 Time delays at peak of cross-correlation of 110° microphone signal and CIP1 combustor pressure signal (in milliseconds)

		Low-pass filter				
Engine power level	No filter	400 Hz	300 Hz	200 Hz	≈150 Hz	100 Hz
48%	94.06	93.83	94.06	94.65	95.29	95.70
54%	93.63	93.90	94.16	94.71	95.12	95.76
60%	93.86	93.67	93.92	94.24	94.54	95.43
71%	94.16	94.24	94.38	94.56	94.77	95.57

Table 3 Peak values of normalized cross-correlation function of 110° microphone signal and CIP1 combustor pressure signal

		Low-pass filter				
Engine power level	No filter	400 Hz	300 Hz	200 Hz	≈150 Hz	100 Hz
48%	0.020	0.210	0.249	0.299	0.341	0.383
54%	0.015	0.181	0.212	0.217	0.201	0.214
60%	0.013	0.155	0.181	0.174	0.146	0.150
71%	0.010	0.128	0.152	0.141	0.115	0.110

Table 4 Time delays at peak of cross-correlation of 160° microphone signal and CIP1 combustor pressure signal (in milliseconds)

		Low-pass filter				
Engine power level	No filter	400 Hz	300 Hz	200 Hz	≈150 Hz	100 Hz
48%	86.58	86.59	86.72	87.17	88.09	88.42
54%	86.46	86.47	86.64	86.91	87.39	87.89
60%	86.21	86.24	86.43	86.49	86.76	87.19
71%	86.90	87.07	87.11	87.16	87.46	88.06

Table 5 Peak values of normalized cross-correlation function of 160° microphone signal and CIP1 combustor pressure signal

Engine power	No	Low-pass	Low-pass	Low-pass	Low-pass	Low-pass
level	filter	400 Hz	300 Hz	200 Hz	≈150 Hz	100 Hz
48%	0.045	0.229	0.254	0.273	0.303	0.324
54%	0.028	0.139	0.158	0.156	0.141	0.147
60%	0.013	0.086	0.092	0.087	0.068	0.062
71%	0.010	0.066	0.072	0.069	0.069	0.071

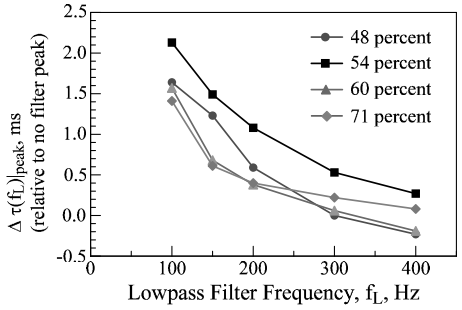

a) 110°

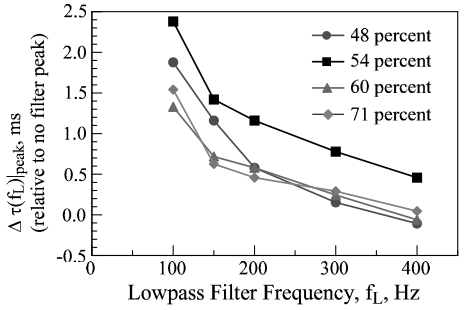

b) 130°

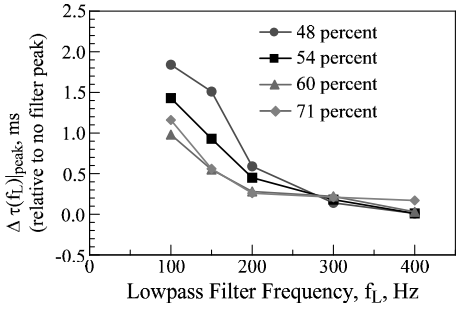

c) 160°

Fig. 9 For far-field microphones at 110, 130, and 160°, comparison of time delay at peak value of the cross-correlation function of low-pass-filtered signals relative to peak time delay using no filter, $\Delta\tau(f_L)|_{\text{peak}}$, as a function of filter design frequency f_L for turbofan engine operating at a setting of 48, 54, 60, and 71% of maximum power.

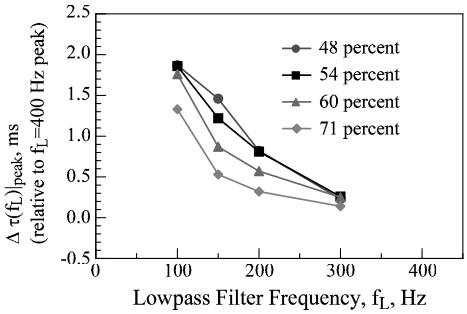

a) 110°

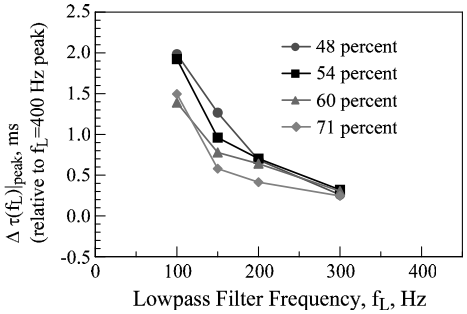

b) 130°

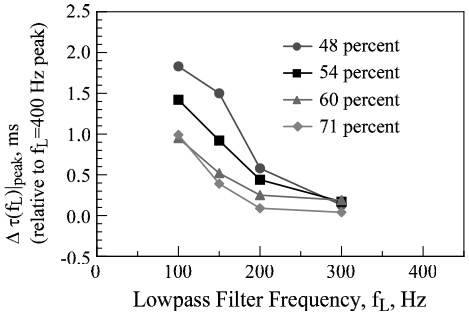

c) 160°

Fig. 10 For far-field microphones at 110, 130, and 160°, comparison of time delay at peak value of the cross-correlation function of low-pass-filtered signals relative to peak time delay using 400 Hz low-pass filter, $\Delta\tau(f_L)|_{\text{peak}}$, as a function of filter design frequency f_L for turbofan engine operating at a setting of 48, 54, 60, and 71% of maximum power.

figures in which the maximum value is maximized and the traces for the 60 and 71% maximum-power cases are similar. In Fig. 10 for each angle the variation of $\Delta\tau(f_L)|_{\text{peak}}$ as a function of f_L for each power setting is shown using the 400 Hz low-pass-filter value as the reference. While the maximum values are lower, the traces for each power setting are more separated.

In Fig. 11 for each power setting the value $\Delta\tau(f_L)|_{\text{peak}}$ as a function of f_L for each angle are shown using the no-filter value as the reference. As the low-pass-filter design cutoff frequency f_L is reduced the time delays tend to increase, because an decreasing amount of direct combustion noise is present. These results show that low-pass filtering can be used to separate this type of dependent source.

In Fig. 12 for each power setting the value $\Delta\tau(f_L)|_{\text{peak}}$ as a function of f_L for each angle are shown using the 400 Hz low-pass-filter value as the reference. Again, as the low-pass-filter design cutoff frequency f_L is reduced the time delays tend to increase, because an decreasing amount of direct combustion noise is present.

The results are more consistent when plotted for each turbofan engine operating setting, as shown in Figs. 11 and 12. The trace of the curves is less dependent on the microphone position and varies depending on operating condition. The major discrepancy is at the 160° angular location for the 54% maximum-power setting when the no-filter reference is used. The grouping of the traces for each angle is a better match when the 400 Hz low-pass-filter peak value is used as a reference. A significant noise source near 1400 Hz produces a significant ripple in the cross-correlation function for this case and makes it difficult to get a valid value for the peak. This ripple is clearly evident in Figs. 6a and 6b.

B. Propagation-Time Evaluation Method

Evaluation of the propagation time using the cross-spectrum between a combustor pressure sensor and a far-field microphone at 100 ft and 130° by Miles [2] indicated that the direct signal had a time delay of 86.98 ms and the indirect signal had a time delay of 90.03 ms. The difference is 3.05 ms, which is attributed to the entropy convecting with the flow before entering the turbine. The linear connection between entropy and pressure fluctuations found by Miles et al. [19] implies that the direct and indirect combustion noise are dependent. The original concept was that the low-frequency core noise source was the combustor and the noise traveled upstream from the combustor through the nozzle. Let the distance the entropy disturbance travels to the turbine entrance be L_c, and let the distance from the turbine entrance to the far-field microphone be r.

Fundamental to the interpretation of the results presented is that entropy waves, or hot spots, travel at the flow velocity, which is only a fraction of the speed of sound. According to Hill and Peterson [20], the average axial velocity of the combustor reactants, v_s, is of the order of 30 m/s. The speed of sound in a combustor, c_c, is generally calculated based on the assumption that the air is a perfect gas [20–22]:

$$c_c = \sqrt{\gamma \Re T_c / W} \tag{5}$$

As reported by Hill and Peterson [20], typical turbine inlet temperatures are of the order of 1600 K. Consequently, the speed of sound c_c is of the order of 800 m/s.

Thus, the direct combustion noise time of travel τ_d is

$$\tau_d = 87.2 \text{ ms} = \frac{L_c}{v_s + c_c} + \frac{r}{c_o} \tag{6}$$

where $L_c = 0.095$ m; $v_s = 30$ m/s; $c_c = 800$ m/s; $r = 30.48$ m; the speed of sound in air is $c_o = 350$ m/s; and the acoustic travel time in the tailpipe, τ_{duct}, is neglected, since it is small and the same for all the sources.

The indirect combustion noise time of travel τ_i is

$$\tau_i = 90.11 \text{ ms} = \frac{L_c}{v_s} + \frac{r}{c_o} \tag{7}$$

Consequently, $\Delta\tau = \tau_i - \tau_d = 3.052 \text{ ms} = L_c(1/v_s - 1/(v_s + c_c))$.

As dependent time histories, these two sources are separated by the cross-spectrum procedure. However, the separation is not as clearly displayed using the cross-correlation method, in which the separation does increase as the filter frequency f_L is reduced but reaches a maximum value near 2.5 ms. This time-delay measurement discrepancy is attributed to difficulties in sufficiently separating the mixture of indirect combustion noise in the 0–200 Hz frequency

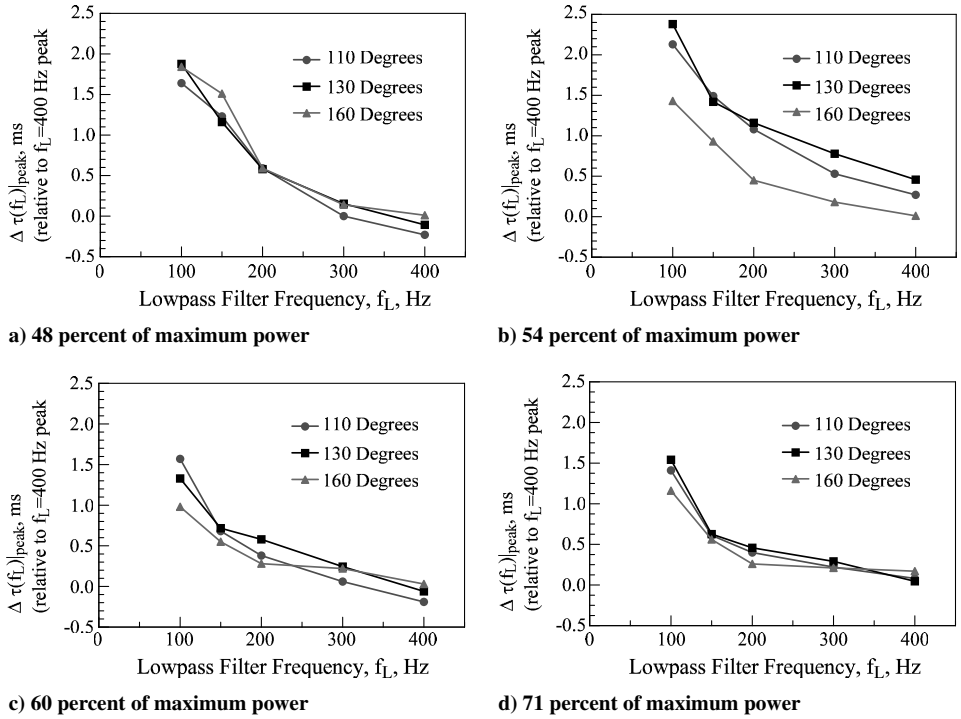

Fig. 11 For far-field microphones at 110, 130, and 160°, comparison of time delay at peak value of the cross-correlation function of low-pass-filtered signals relative to peak time delay using no filter, $\Delta\tau(f_L)|_{\text{peak}}$, as a function of filter design frequency f_L for turbofan engine operating at a setting of 48, 54, 60, and 71% of maximum power.

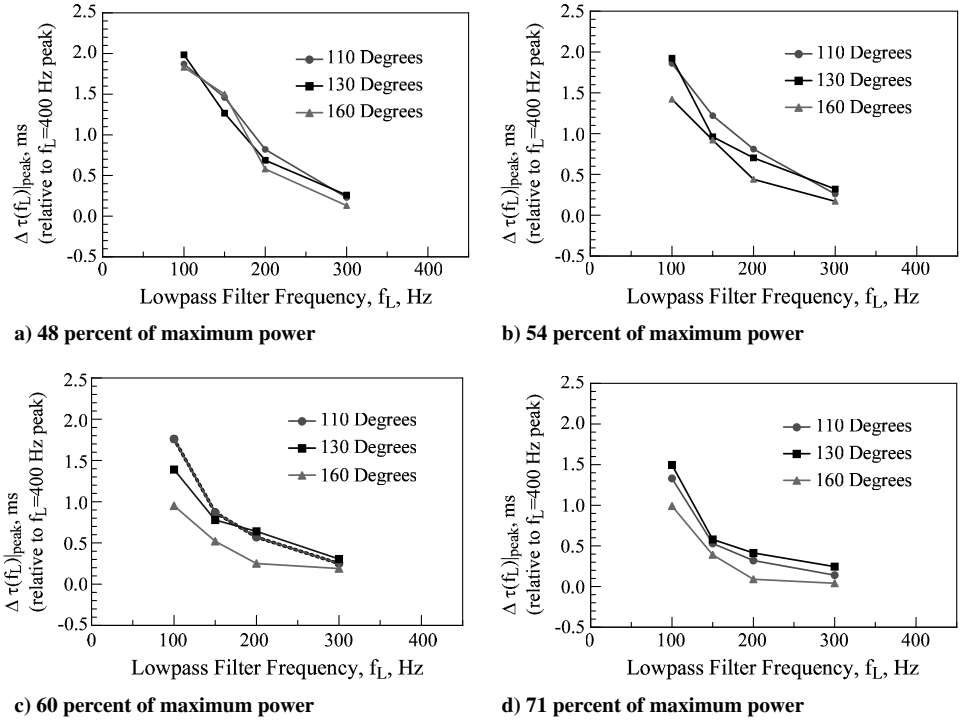

a) 48 percent of maximum power

b) 54 percent of maximum power

c) 60 percent of maximum power

d) 71 percent of maximum power

Fig. 12 For far-field microphones at 110, 130, and 160°, comparison of time delay at peak value of the cross-correlation function of low-pass-filtered signals relative to peak time delay using 400 Hz filter, $\Delta\tau(f_L)|_{\text{peak}}$, as a function of filter design frequency f_L for turbofan engine operating at a setting of 48, 54, 60, and 71% of maximum power.

range from the direct combustion noise in the 200–400 Hz frequency range. This problem also appears in results obtained by Miles [1] using the 150 Hz low-pass-filtered signals with the cross-spectrum method. It can be seen in Figs. 15 and 16 of that paper that the use of a time delay of 86.98 ms creates a flat phase angle between 200–300 Hz shown in Fig. 16(c), indicating this is the direct combustion noise location (fast propagation speed), while using a time delay of 90.03 ms creates a flat phase angle between 0–200 Hz shown in Fig. 15(c), indicating this is the indirect combustion noise location (slow propagation speed). Using this 150 Hz low-pass filter still leaves the signals so intermixed that one is barely able to distinguish between direct and indirect combustion noise. In addition, as the low-pass-filter frequency is reduced, the cross-correlation peaks in the time domain get wider.

Identifying the sources creating a system output signal is generally achieved using specific tagged input test signals. For the turbofan engine combustion noise problem, this is difficult and we must depend currently on tagged signals created by the system. Consequently, using the cross-correlation procedure or the low-pass-filtering procedure, we arrive at viewing the output signal as being a blend of indirect combustion noise (which is loudest in the 0–200 Hz frequency range and has a longer propagation time to the far field) and direct combustion noise (which is loudest in the 200–400 Hz frequency range and has a quicker propagation time to the far field). However, the indirect and direct combustion noise source frequency ranges overlap for this engine and, as a consequence, low-pass filtering as implemented herein is not as useful as one would hope in separating the direct and indirect combustion noise. One needs a way to study the blending as a function of frequency. However, these results do show that low-pass filtering can be used with the cross-correlation function to separate this type of dependent source to some extent and confirm the cross-spectrum results. The fact that both methods do create separation to some extent gives credence to the hypothesis that the far-field low-frequency core noise is due to a blend of direct and indirect combustion noise for this engine. Detailed information on how the signals are blended or mixed as a function of frequency is not available and must be the subject of further investigation. In addition, it might be a function of engine design as well as operating condition. Determining the mixture or blend as a function of frequency of direct and indirect combustion noise is an important research objective. However, the first step is to show that an indirect combustion noise source is responsible for part of the far-field turbofan engine noise spectrum.

C. Identification of Combustion Noise

As previously shown by Miles [1] using the 130° far-field microphone, Tables 3 and 5 show the use of a sequence of low-pass filters to study the cross-correlation of the noise from the CIP1 sensor, and the far-field microphones show that filtering can increase the correlation function significantly. A low-pass filter in the range of 200–300 Hz works well for this particular turbofan engine.

V. Conclusions

Low-pass filtering with a 100 Hz cutoff frequency to remove a large amount of the direct combustion noise leaves the indirect combustion noise, which has a relative time delay of approximately 1–2.5 ms. This time delay is longer than the time delay observed with no filtering or low-pass filtering at 400 Hz. This shows some of the direct combustion noise, which is always traveling at the speed of sound has been removed, leaving the indirect combustion noise, which spends some time moving convectively at a much lower velocity than the speed of sound in the combustor. As a consequence of removing part of the combustion noise that travels fastest, the delay time of the combustion noise remaining in the signal is greater. The largest indirect combustion noise time delay found using this procedure is about 2 ms. The cross-correlation function, when used with low-pass filtering, is very useful in separating the indirect and direct combustion noise source in this system.

Coherence analysis using the cross-spectrum phase-angle method separates direct and indirect combustion noise using filtered or unfiltered signals. This is done by an examination of the effect of using different time delays has on the phase angle of the cross-spectrum calculated using the combustor pressure sensor signal and a far-field microphone signal. For the cross-spectrum between a combustor pressure sensor and a far-field microphone at 130°, this method indicated that the direct signal had a time delay of 86.98 ms

and the indirect signal had a time delay of 90.03 ms. The indirect combustion noise time-delay time is thus 3.05 ms.

This time-delay measurement discrepancy is attributed to difficulties in sufficiently separating the mixture of indirect combustion noise in the 0–200 Hz frequency range from the direct combustion noise in the 200–400 Hz frequency range. In addition, as the low-pass-filter frequency is reduced, the cross-correlation peaks in the time domain get wider. These results show that low-pass filtering can be used with the cross-correlation function to separate this type of dependent source to some extent and confirm the cross-spectrum results.

For the 48% of maximum-power case, two peaks separated by 4–4.5 ms were measured. If these peaks are due to direct and indirect combustion noise, this would show that some of the direct combustion noise (which is always traveling at the speed of sound) is responsible for the peak at the shortest time, and the indirect combustion noise (which spends some time moving convectively at a much lower velocity than the speed of sound in the combustor) is responsible for the peak at the longer time.

Examination of the results using the three different far-field microphones shows that the time delays measured at each angle are fairly consistent with one another at a given operating condition. The results may lead to a better idea about the acoustics in the combustor and may help develop and validate improved reduced-order physics-based methods for predicting direct and indirect combustion noise.

References

[1] Miles, J. H., "Core Noise Diagnostics of Turbofan Engine Noise Using Correlation and Coherence Functions," *Journal of Propulsion and Power*, Vol. 26, No. 2, March–April 2010, pp. 303–316. doi:10.2514/1.42980

[2] Miles, J. H., "Spectral Separation of the Turbofan Engine Coherent Combustion Noise Component," AIAA Paper 2008-50, Jan. 2008; also NASA TM-215157-0, 2008.

[3] Miles, J. H., "Time Delay Analysis of Turbofan Engine Direct and Indirect Combustion Noise Sources," *Journal of Propulsion and Power*, Vol. 25, No. 1, Jan.–Feb. 2009, pp. 218–227. doi:10.2514/1.38030

[4] Mendoza, J. M., Nance, D. K., and Ahuja, K. K., "Source Separation from Multiple Microphone Measurements in the Far Field of a Full Scale Aero Engine," AIAA Paper 2008-2809, 2008.

[5] Weir, D. S., and Mendoza, J. M., "Baseline Noise Measurements from the Engine Validation of Noise and Emissions Reduction Technology Program," AIAA Paper 2008-2807, 2008.

[6] Schuster, B., "Statistical Considerations for Gas Turbine Engine Noise Measurements," AIAA Paper 2008-2808, 2008.

[7] Royalty, C. M., and Schuster, B., "Noise fro a Turbofan Engine Without a Fan from the Engine Validation of Noise and Emission Reduction Technology (EVNERT) Program," AIAA Paper 2008-2810, 2008.

[8] Dougherty, R. P., and Mendoza, J. M., "Nacell In-Duct Beamforming Using Modal Steering Vectors," AIAA Paper 2008-2812, 2008.

[9] Weir, D. S. (ed.), "Engine Validation of Noise & Emission Reduction Technology Phase 1," NASA CR-2008-215225, May 2008.

[10] Hultgren, L., and Miles, J., "Noise-Source Separation Using Internal and Far-Field Sensors for a Full-Scale Turbofan Engine," 15th AIAA/CEAS Aeroacoustics Conference, AIAA Paper 2009-3220, Miami, FL, May 2009.

[11] Carter, G. C., "Tutorial Overview of Coherence and Time Delay Estimation," *Coherence and Time Delay Estimation*, edited by G. C. Carter, Part 1, IEEE Press, Piscataway, NJ, 1993, pp. 1–27.

[12] Scarbrough, K., Ahmed, N., and Carter, G. C., "On the Simulation of a Class of Time Delay Estimtion Algorithms," *IEEE Transactions on Acoustics, Speech, and Signal Processing*, Vol. 29 No. 3, pt. 2, June 1981, pp. 534–540. doi:10.1109/TASSP.1981.1163615

[13] Bendat, J. S., and Piersol, A. G., *Random Data: Analysis and Measurement Procedures*, Wiley, New York, 1971.

[14] Bendat, J. S., and Piersol, A. G., *Engineering Applications of Correlation and Spectral Analysis*, Wiley, New York, 1980.

[15] Stearns, S. D., and David, R. A., *Signal Processing Algorithms Using Fortran and C*, Prentice–Hall, Upper Saddle River, NJ, 1993.

[16] Kormylo, J. J., and Jain, V. K., "Two-Pass Recursive Digital Filter with Zero Phase Shift," *IEEE Transactions on Acoustics, Speech, and Signal Processing*, Vol. 22, No. 5, Oct. 1974, pp. 384–387. doi:10.1109/TASSP.1974.1162602

[17] Hamming, R. W., *Digital Filters*, 3rd ed,, Dover, Mineola, NY, 1989, p. 252.

[18] Matsumoto, M., and Nishimura, T., "Mersenne Twister: A 623-Dimensionally Equidistributed Uniform Pseudo-Random Number Generator," *ACM Transactions on Modeling and Computer Simulation*, Vol. 8, No. 1, Jan. 1998, pp. 3–30. doi:10.1145/272991.272995

[19] Miles, J. H., Wasserbauer, C. A., and Krejsa, E., "Cross Spectra Between Temperature and Pressure in a Constant Area Duct Downstream of a Combustor," Paper AIAA Paper 83-0762, 1983; also NASA TM-83351, 1983.

[20] Hill, P. G., and Peterson, C. R., *Mechanics and Thermodynamics of Propulsion*, 2nd edition, Addison-Wesley, Reading, MA, 1992.

[21] Poinsot, T., and Veynante, D., *Theoretical and Numerical Combustion*, 2nd edition, R. T. Edwards, Philadelphia, 2005.

[22] Lieuwen, T. C., and Yang, V., *Combustion Instabilities in Gas Turbine Engines: Operational Experience, Fundamental Mechanisms, and Modeling*, AIAA, Reston, VA, 2005.

K. Frendi
Associate Editor